A Monolithic Polyimide Micro Cryogenic Cooler: Design, Fabrication, and Test

Yunda Wang, Ryan Lewis, Ray Radebaugh, Martin M.-H. Lin, Victor M. Bright, *Senior Member, IEEE*, and Yung-Cheng Lee, *Senior Member, IEEE*

***Abstract*— In this paper, we present the design, fabrication, and testing of a monolithic polymer Joule–Thomson microcryogenic cooler (MCC) cold stage. The MCC cold stages were fabricated monolithically on a wafer out of polyimide. The fabrication was based on surface micromachining technologies using electroplated copper as the sacrificial layers and polyimide as the structural material. The process consisted of multilayers of metallization, coating of polyimide, and the patterning on each layer. One of the key techniques enabling this monolithic approach was the development of the wafer-level 3-D interconnect for making high pressure (e.g., 10 atm) polymer fluid microchannels. To evaluate the performance of the MCC, a five-component fluid mixture designed for cooling from 300 to 200 K was used as a refrigerant. The cold tip reached 190 K under a refrigerant pressure ratio of 6.2:1.1 bar. The heat-lift at 200 K was measured to be 5.2 mW. [2013-0211]**

***Index Terms*— Micro cryogenic cooler, polyimide, monolithic, 3-D interconnect, mixed refrigerant, fluid micro channels, wafer-level process.**

I. Introduction

MICRO CRYOGENIC COOLERS (MCC) are intended to cool low power-consumption sensors thereby lowering thermal noise, enhancing bandwidth, and enabling superconductivity in the sensor [1]. In recent decades, the miniaturization of Joule-Thomson (J-T) coolers has attracted considerable interest and shown a great potential for small size, low noise, fast response, and high efficiency cryogenic cooling applications. With the same heat lift, a J-T MCC's power input can be as little as 1/10th of a thermoelectric cooler's input, and it's size can be as little as 1/10th of a Stirling cooler's size [2].

Fig. 1 shows the system schematics and operation principle of the J-T micro cryogenic cooler. Refrigerant flows continuously through the compressor, heat exchanger (high-pressure channels), J-T expansion valve (or an orifice), evaporator, heat exchanger (low-pressure channels), and then through the compressor again forming a closed loop cycle. The gas mixture (refrigerant) is pressurized by a compressor (Fig. 1, a→b), and then it flows through a cooler to be precooled (Fig. 1, b→b'). After precooling, the gas mixture flows through a counter-flow heat exchanger, where it exchanges heat with the gas flowing in the opposite direction inside the low-pressure line (Fig. 1, b'→c). When the gas mixture meets a flow restriction (Fig. 1, J-T orifice), it undergoes an isenthalpic expansion and the pressure drops from high to low. During the expansion process, the gas mixture cools and can undergo partial or complete phase change (Fig. 1, c→d). Some liquid components evaporate or boil while absorbing heat from the device and from the environment (Fig. 1, d→e). From the cold end, the low-pressure two-phase fluid flows back into the heat exchanger (Fig. 1, e→a) to cool the incoming high-pressure warm fluid for enhancement of efficiency. The gas eventually goes back to the compressor system to complete a closed-loop Joule-Thomson cooling cycle. The term "MCC" in this paper is to indicate the cold-stage part of the J-T micro cryocooler system only containing the J-T valve and the heat exchanger as illustrated in Fig. 1.

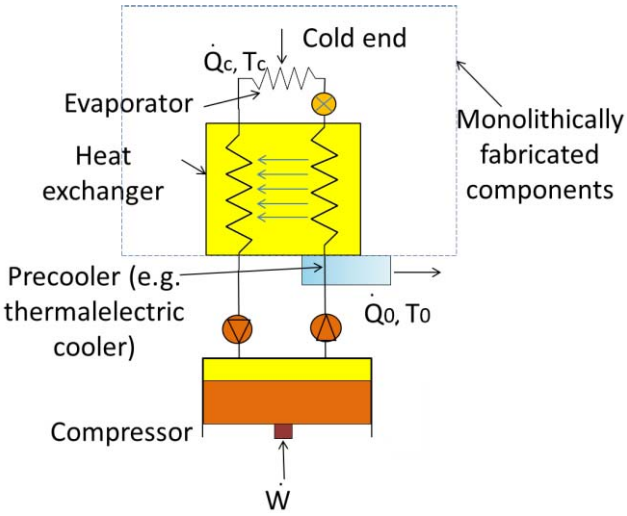

Fig. 1. Schematics of the operation principle of the J-T micro cryocooler system.

In the 1980s, W. Little *et al.* [3], [4] made a series of matchbox-sized J-T MCCs based on an etched glass

Manuscript received July 3, 2013; revised November 19, 2013; accepted January 12, 2014. Date of publication February 12, 2014; date of current version July 29, 2014. This work was supported in part by the Defense Advanced Research Projects Agency Micro Cryogenic Cooler Program under Grant NBCHC060052 and Grant W31P4Q-10-1-0004, and in part by the Nanotechnology Infrastructure Network at the Colorado Nanofabrication Laboratory. Subject Editor L. Lin.

Y. Wang is with Palo Alto Research Center, Palo Alto, CA 94304 USA (e-mail: yundawangyd@gmail.com).

R. Lewis, V. M. Bright, and Y.-C. Lee are with the Department of Mechanical Engineering, University of Colorado at Boulder, Boulder, CO 80309 USA (e-mail: ryan.j.lewis-1@colorado.edu; victor.bright@colorado.edu; leeyc@colorado.edu).

R. Radebaugh is with the National Institute of Standards and Technology, Boulder, CO 80305 USA (e-mail: radebaugh@boulder.nist.gov).

M. M.-H. Lin is with Symmetricom Inc., Beverly, MA 01915 USA (e-mail: muhongcolorado@yahoo.com).

Color versions of one or more of the figures in this paper are available online at http://ieeexplore.ieee.org.

Digital Object Identifier 10.1109/JMEMS.2014.2301631

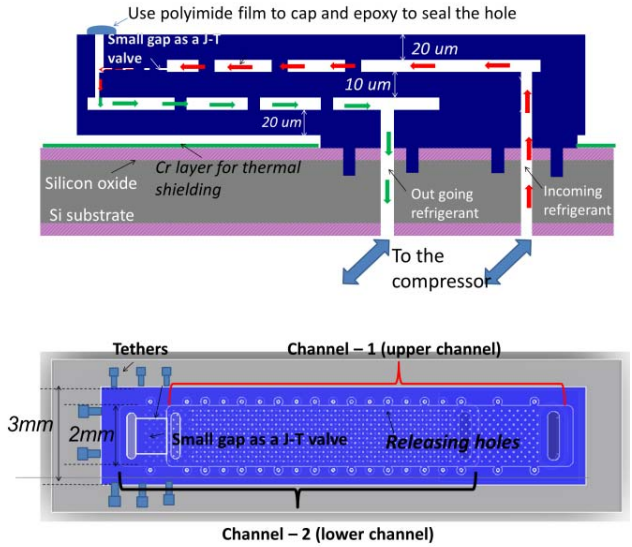

Fig. 2. The cross-sectional view and the top view of the monolithic polyimide MCC.

plate heat exchanger. The lowest temperature ranged from 88 K to 70 K. In 2001, J. Burger *et al.* [5] reported a 77 mm × 9 mm MCC using a coaxial heat exchanger formed with glass capillary tubes. In 2006, Lerou *et al.* [6] fabricated a 30 mm × 2.2 mm glass plate based J-T cooler that reached 100 K. M.-H. Lin et al. [1], [7] inserted six hollow-core glass fibers (ID/OD=75μm/125μm) into a larger glass capillary tube (ID/OD=536μm/617μm), forming a tubes-in-tube counter flow heat exchanger for a MCC.

In 2012, a planar polymer-based MCC which consisted of a micro machined polyimide counter flow heat exchanger and a silicon/glass based J-T expansion valve had been developed at the University of Colorado at Boulder and NIST as reported in [8] and [9]. Compared to the previous works on MCC, most of the fabrication processes were achieved on wafer-level which substantially enhanced the manufacturability and scalability. However, in such a design, a J-T valve and a heat changer were made separately to achieve such a complicate 3-D micro fluid system, and solder assembly method was used in order to make a 3-D connection of the channels of the heat exchanger with J-T valve. It confined the manufacturability and yield of the device due to a non-monolithic process. A mechanical leakage problem has been identified in the bonding interface of the device, therefore the flow rate (260 sccm) was much higher than expected design number (10 sccm) making the performance worse than the design target [9]. The major reason for the performance degradation was because with such a high flow rate, the heating exchange between the two lines of the heat exchanger degraded dramatically and refrigeration loss due to pressure drop along the heat exchanger became too high.

The development of the polyimide-based MCC was continued as a joint effort at the University of Colorado at Boulder and NIST. In this paper, the MCC assembly method has been replaced by a new approach by making monolithic polyimide MCCs as presented in Fig. 2. The new MCCs cold stage including a heat exchanger and a J-T valve were all fabricated monolithically on a wafer all using polyimide. Compared to the assembly-based approach, this monolithic polyimide MCC did not encounter the mechanical leakage problem since the soldered-interface was removed. It also further enhanced the manufacturability and scalability of the MCC through the wafer-level processing. The cold end temperatures were improved from 233 K to 190 K with a flow rate reduced from more than 260 standard cubic centimeters per minute (sccm) to 62 sccm. The cryogenic demonstration was accomplished by using a custom 5 components refrigerant (8% methane, 46% ethane, 14% propane, 4% butane and 26% pentane with respect to molar fraction) designed by scientists in NIST. The optimization was targeting for a 300k to 200K cooling under a flow rate of 10 sccm and operating pressures of 4 bar and 1 bar for high and low pressure sides.

II. System Design and Optimization

Fig. 2 shows the cross-sectional view and the top view of the monolithic polyimide MCC. It consisted of a micro machined polyimide heat exchanger and Joule-Thomson (J-T) expansion valve. The heat exchanger had a structure consisting of two parallel rectangular polyimide channels stacked on top of each other. On the cold end, the two heat exchanger channels were interconnected with a polyimide gap of 3.4 μm, while on the warm end they were connected to the fluid via holes on the silicon substrate going to compressors thereby forming a Joule-Thomson loop. Polyimide posts were used to strengthen the polyimide fluid channels that have been proven reliable for a 10-atm gas flow. The polyimide MCC's dimensions were 15 mm × 3 mm × 90 μm with one of the ends tethered for both excellent thermal isolation and good mechanical properties.

The ideal cooling power of a refrigerant in a J-T cryogenic cooler is given by the product of flow-rate with the minimum isothermal enthalpy difference between the high-pressure refrigerant and low-pressure refrigerant [10].

$$\dot{Q}_r = \dot{n}(\Delta h|_T)_{min} \tag{1}$$

where $\dot{Q}_r$ is the gross refrigeration delivered by the mixed refrigerant pumped by the compressor; $\dot{n}$ is the flow rate in mol/s; $(\Delta h|_T)$ is the minimum molar isothermal enthalpy difference of the refrigerants between the high pressure and low pressure enthalpies within the temperature range of interest.

However, in a the realistic situation, there will be refrigeration losses associated with imperfect heat transfer, pressure drop, and environment heating as given in equation (2) [11],

$$\dot{Q}_{net} = \dot{Q}_r - \dot{Q}_{\Delta p} - \dot{Q}_{HX} - \dot{Q}_{cond} - \dot{Q}_{rad} \tag{2}$$

where $\dot{Q}_{\text{net}}$ is the net refrigeration (heat lift) of the MCC; $\dot{Q}_{HX}$ is refrigeration loss due to heat exchanger ineffectiveness; $\dot{Q}_{\Delta p}$ is the refrigeration loss resulting from the pressure drop along the heat exchanger; $\dot{Q}_{\text{cond}}$ is the conduction heat load through the heat exchanger or DC leads used to power the device; and $\dot{Q}_{\text{rad}}$ is the radiation heat load from the environment. Calculations of each of the components have been elaborated by Radebaugh in [11]. Since the cold stage was operated in a vacuum chamber with air pressure less than 10^{-4} Torr, conduction heat load through the air was negligible.

TABLE I
KEY DIMENSIONS OF MCCS

Parameters	*Values*
Thickness of the top layer of the channel, t_{top}	20 μm
Thickness of the bottom layer, t_{bottom}	20 μm
Thickness of the center layer, t_{center}	10 μm
Diameter of the posts, d_{post}	60 μm
Space between the post, S_{posts}	150 μm
Length of the channels, L_c	12 *mm*
Width of the channels, W_c	2 *mm*
Height of the channels, Gc	30 μm
Width of the heat exchanger including sealing edge, W_{HX}	3 *mm*
Gap of the J-T valve, G_{JT}	3.4 μm
Length of the J-T valve, L_{JT}	1.8 *mm*
Width of the J-T valve, W_{JT}	1.7 *mm*

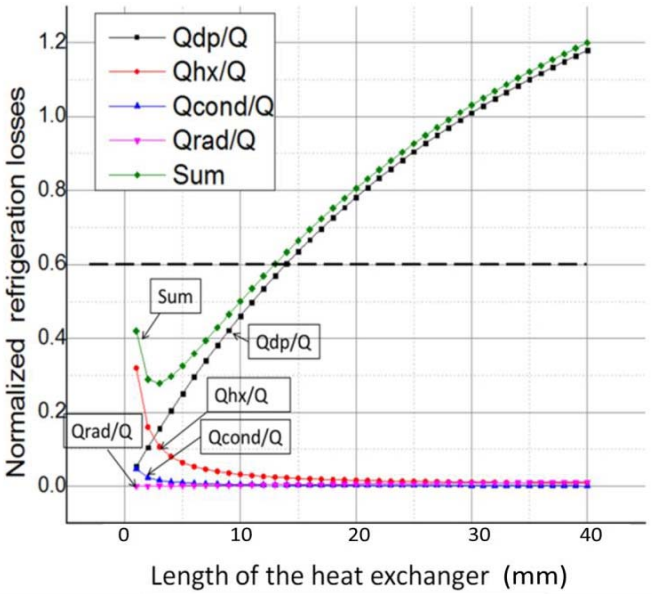

Fig. 3. The ratio of the refrigeration losses to the total gross refrigeration power. Each refrigeration loss was calculated according to the method presented in [10].

The heat exchanger optimization has been elaborated in [9] for the polyimide-based MCC. The results were directly applicable here. The only difference was that the silicon/glass J-T valve was replaced with a polyimide J-T valve integrated with the heat exchanger, and the J-T valve was a polyimide gap of 3.4 μm. In such a case, the typical key dimensions of the monolithic MCC can be found in Table I.

Fig. 3 shows an example of normalized losses of the refrigeration power versus the length of the heat exchanger. The calculation was done under the assumption of using the optimized mixed refrigerant as described in Section I. The design was considered reasonable as far as the ratio of the refrigeration loss to the total refrigeration power was less than 60% which means at least 40% of the gross refrigeration power was successfully used, as has been noted as a practical limit based on experimental experience [11].

III. THERMAL ISOLATION OF MCC

Environmental and parasitic heat load is one of the major refrigeration losses of the MCC. Due to the high surface-to-volume ratio and short path for heat conduction from the worm end to the cold end, the heat leak from the environment (radiation and conduction losses) is particularly significant in the micro cryogenic cooler with limited gross refrigeration power. High thermal isolation design is essential to manage the heat losses and increase the net refrigeration power for a given gross refrigeration power.

In the previous MCC studies, one solution was to increase the gross refrigeration power to compensate the loss to environment. In Little's work [3], [4], [12], and [13], high gross refrigeration powers were reached by using relative high pressure ratio nitrogen (16.5:0.1 MPa) and flow-rate (107 μmol/s). In University of Twente's work [14] and [15], a low emissivity metal thin film was coated on the heat exchanger to reduce its radiation loss, however, a much higher pressure (8 MPa) and flow-rate were used in order to compensate the loss. Clearly the thermal isolation is extremely important for such a small size micro cryogenic cooler with limited gross refrigeration (30.3 mW gross refrigeration at 10 sccm flow rate using equation 1).

In this work, it is important to understand contribution of each part of the MCC to the thermal refrigeration losses for reasonable thermal isolation design; e.g. by knowing the radiation loss of each part, one can decide how important it is to coat reflective shielding for some part. In addition, tethers are used to make a mechanical support of the MCC. Their contribution to refrigeration loss was not considered in the optimization in section II. Tethers' design do not affect the functional part of the heat exchanger while on the other hand, it is a trade-off design between the thermal losses and mechanical design, so it is more convenient to isolate the thermal analysis of the tethers from the optimization of the heat exchanger.

In the MCC, heat was transferred from the environment to the cold end by conduction and radiation. The conduction loss therefore was mainly due to the heat transfer along the solid parts of the MCC since the heat transfer through air was considered negligible due to the very low air pressure of the chamber. This can be expressed by Fourier's law of heat conduction as equation (3) [16]

$$\dot{Q}_{cond} = kA\frac{\partial T}{\partial x} \tag{3}$$

where $\dot{Q}_{cond}$ is the heat transfer rate, A is the cross sectional area, T is the temperature, x is the length along the temperature gradient and k is the thermal conductivity (from 0.186 W $\cdot$ m^{-1} $\cdot$ K^{-1} at 300K to 0.175 W $\cdot$ m^{-1} $\cdot$ K^{-1} at 200K [17], 0.18 W $\cdot$ m^{-1} $\cdot$ K^{-1} was used as an average value) of the material. For a heat exchanger of which the cross-sectional area does not change along the direction, the

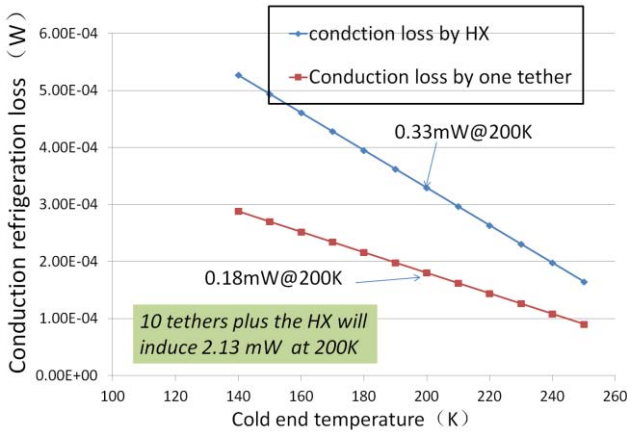

Fig. 4. Refrigeration losses due to conduction. (Under the assumption that radiation heat transfer to the environment can be ignored compared to the conduction heat transfer.)

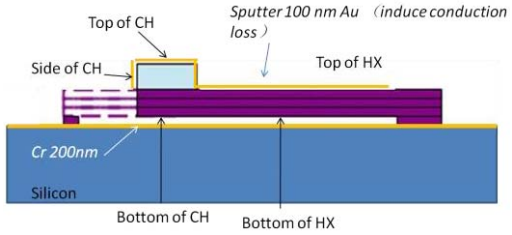

Fig. 5. Shielding methods of the MCC.

temperature along the length direction can be treated as a liner distribution. However, the assumption is right only if the radiation heat transfer to the environment can be ignored compared to the conduction heat transfer. In our calculation, the area of tethers is very small and also we assumed that the heat exchanger is well shielded using reflective coatings as what is shown is in Fig. 5, so that the radiation compared to the conduction is negligible. Under such an assumption, we can quickly estimate the conductive refrigerant loss along the tethers and along the heat exchanger if we make good shielding on it. Conduction refrigeration losses along a well shielded heat exchanger (with dimensions shown in Table I) and tethers (with a typical dimension of L × W × H = 300 × 60 × 50 μm) are shown in Fig. 4 for an interested cold end temperature range (from 140 K to 250 K).

The radiation heat transfer from an ideal thermal radiator, or a black body, can be modeled by the Stefan-Boltzmann law of thermal radiation [16]

$$\dot{Q}_{\text{rad}} = \varepsilon_{\text{eq}} A(T_2^4 - T_2^4) \ \ for \ \ T_2 \geq T_1 \tag{4}$$

where σ is the Stefan-Boltzmann constant with the value of 5.669E-8 W/m^2 · K. A is the surface area of the radiator, T_1 is the temperature of the radiator and T_2 is the temperature of the environment material, ε_{eq} is the equivalent emissivity which is determined by emissivity of the radiator (ε_1) and environment material (ε_2) and their geometries. For example, for $A_2 \gg A_1$, $\varepsilon_{\text{eq}} \doteq \varepsilon_1$; for an infinite parallel plates structure $\varepsilon_{\text{eq}} = 1/\ (1/\varepsilon_1 + 1/\varepsilon_2 - 1)$.

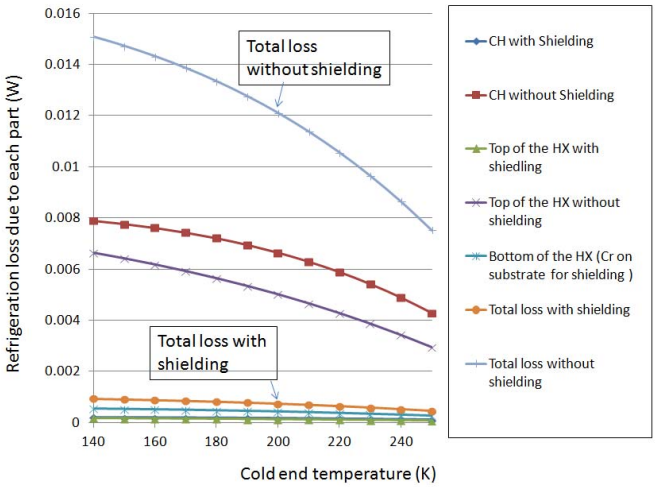

Fig. 6. Radiation refrigeration energy loss of the MCC.

On the silicon substrate, a 100 nm thin Cr layer was coated in order to minimize the radiation from the environment to the bottom of the MCC. The heat exchanger was very close (15 μm) to the Cr coated silicon substrate therefore it was considered well shielded. The upper side of the heat exchanger was not coated with low emissivity material. However, further shielding of the upper side of the heat exchanger can be achieved by sputtering metal layer, for example, a gold layer with 100 nm in thickness, to dramatically decrease the emissivity of the surface. Fig. 5 illustrates the potential shielding method that can be achieved by coating Cr on the Si substrate and sputtering Au on other exposed areas.

Radiation refrigeration losses due to different parts with and without potential shielding method were then calculated according to a cold head desired temperature range from 140K to 250K (see Fig. 6). In Fig. 5, we have introduced an extra volume of cold head (CH) with a footprint of 2 mm × 3mm and 0.9 mm in thickness to simulate a device that will be attached, e.g. a sensor chip to be cooled. The result indicates that, with a thin layer of metal coating to cover the CH top and sides, about 6 mW extra heat lift can be achieved without adding any extra conduction loss. If we metalize the top surface of the heat exchanger with 100 nm Au, the total radiation loss can be reduced dramatically with only adding much smaller extra conduction loss. For example, in our case, the MCC's radiation loss can be reduced by 5.27mW with only inducing 1.16 mW of conduction loss for a 200 K cold end temperature condition. Thus, we can benefit significantly from the shielding by reducing the radiation loss exponentially. In the demonstration which is shown in section V, the CH was shielded with metal tapes which have similar emissivity to gold. In this case, the radiation refrigeration losses were reduced by 6 mW.

IV. Fabrication of MCC

Properties of polyimide have been well studied at cryogenic temperature, and they show it is a good candidate polymer for cryogenic applications [18], [19]. It has high stability even at cryogenic temperature, e.g., with decreasing temperature

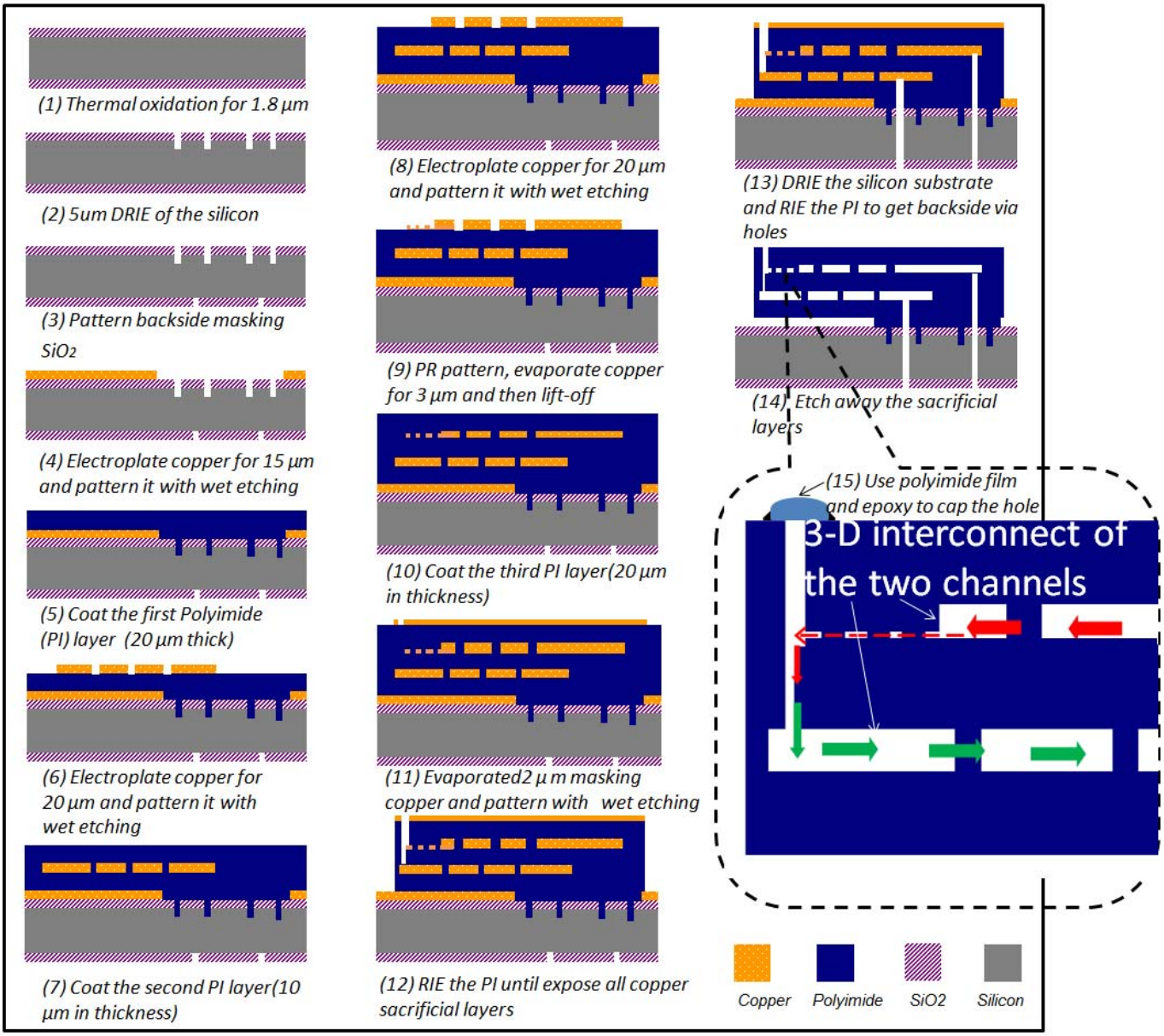

Fig. 7. Fabrication process flow of the monolithic polyimide MCC.

from room temperature to 4.2 K, the failure strain of a typical polyimide continuously decreases by only 25%, and the fracture toughness increases continuously by 10% [18]. Electroplated copper has been used as a sacrificial layer to make suspended polyimide structures [20], [21]. Here we fabricate the heat exchanger by using multiple suspended polyimide layers based on this technology and combine it with silicon bulk micromachining.

The process to fabricate the monolithic polyimide MCC consists of multi-layers of metallization of copper, spin coating and curing of polyimide, and the patterning of each layer. By properly overlapping and aligning the copper sacrificial layers, a final go-through etching is able to selectively connect the different channel or gap in different layers. The detailed steps and their explanations are as follows and illustrated in Fig. 7.

(1) A masking oxide approximately 1.5 μm thick was grown on both sides of a Si wafer with wet thermal oxidation.

(2) O-ring shaped trenches were patterned in the SiO_2 layer using reactive ion etching (RIE), followed by 5 μm deep reactive ion etching (DRIE) of silicon with silicon oxide as a mask. The trenches are to enhance the bonding and sealing of the fluid interface between the polyimide layer and silicon substrate.

(3) Backside SiO_2 was patterned utilizing RIE. This patterning is to prepare mask for later backside DRIE etching.

(4) An adhesion layer of chromium 100 nm in thickness followed by an electroplated seed layer of copper 500 nm in thickness were evaporated onto the wafer using a thermal evaporator. Additional copper of 15 μm was electroplated with a current density of approximately 10 mA/cm^2. The metals are then patterned with wet etching serving as the first sacrificial layer.

(5) Polyimide (DuPont PI-2611*) was then deposited onto the wafer in two spin coats of 2000 rpm for 30 seconds

followed by a soft bake after each coat at 100 °C for 120 seconds. After all the spin coats, the polyimide was cured at 260 °C for 1 hour in nitrogen, resulting in an after- cure thickness of 20 μm.

(6) Similar to (4) but using an adhesion layer of 10 nm thick titanium, instead of using chromium, followed by a 400 nm thick copper electroplating seed layer were deposited using a thermal evaporator. Additional copper of 20 μm was then electroplated followed by patterning to the geometry as one of the later embedded micro channels in the heat exchanger. The patterning of copper and titanium were done by using wet etching and RIE in a plasma of CF_4:O_2 ratio of 4:16 respectively.

(7) A second polyimide (DuPont PI-2611) layer was spin coated at 2000 rpm for 30 seconds followed by a soft bake at 100 °C for 120 seconds and cured at 260 °C for 1 hour in nitrogen, yielding a thickness of about 10 μm.

(8) Same to (6), another 20 μm thick layer of copper plating and wet etching were done to form the geometry of the other embedded micro channel in the heat exchanger.

(9) Photoresist of 10 μm thick was deposited on to the wafer and patterned to expose the J-T valve area followed by thermally evaporating 10 nm Ti and 3.4 μm thick copper. The metal layers are then patterned with lift-off by the photoresist serving as a sacrificial layer for forming the J-T valve.

(10) The exact same process as described in (5) was done again to form another polyimide layer 20 μm in thickness.

(11) A hard metal mask of 10 nm of titanium (as the adhesion layer) and 2.5 μm of copper was evaporated on the polyimide layer. It was then patterned to the geometry of the HX with alignment entrance and exit holes on the end and releasing holes along the sealing edge of the heat exchanger.

(12) The exposed polyimide was etched in a CF_4 and O_2 (CF_4:O_2 = 6:10 sccm) plasma down to the copper metal to expose all the sacrificial Cu layers, including the bottom sacrificial layer, lower channel sacrificial layer and the J-T valve sacrificial layer. At this point, the lower channel was then connected to the J-T valve. Because the metal defining the J-T valve is already connected to the upper channel sacrificial layer, three of them should be able to be connected together after releasing the sacrificial Cu.

(13) Backside entrance and exit holes were etched from the backside of the substrate using DRIE. Further RIE in a CF_4 and O_2 (CF_4:O_2 = 6:10 sccm) plasma was then done to etch the polyimide making the entrance and exit holes go all the way to their channels filled with metal.

(14) The sacrificial layers of copper were etched away at the end in a standard copper etchant (Transene CE-100) at 60°C forming the embedded micro channels in the MCC and free the whole MCC structure. The etch time to fully release the structure was approximately 48 hours.

(15) A Kapton film was used as a cap and is epoxy-glued to seal the top etching holes on the cold tip.

Finally epoxy applicable for cryogenic applications was used to fill the releasing holes after the device was released. Figs. 8 and 9 show the photos and SEM pictures of the fabricated MCCs.

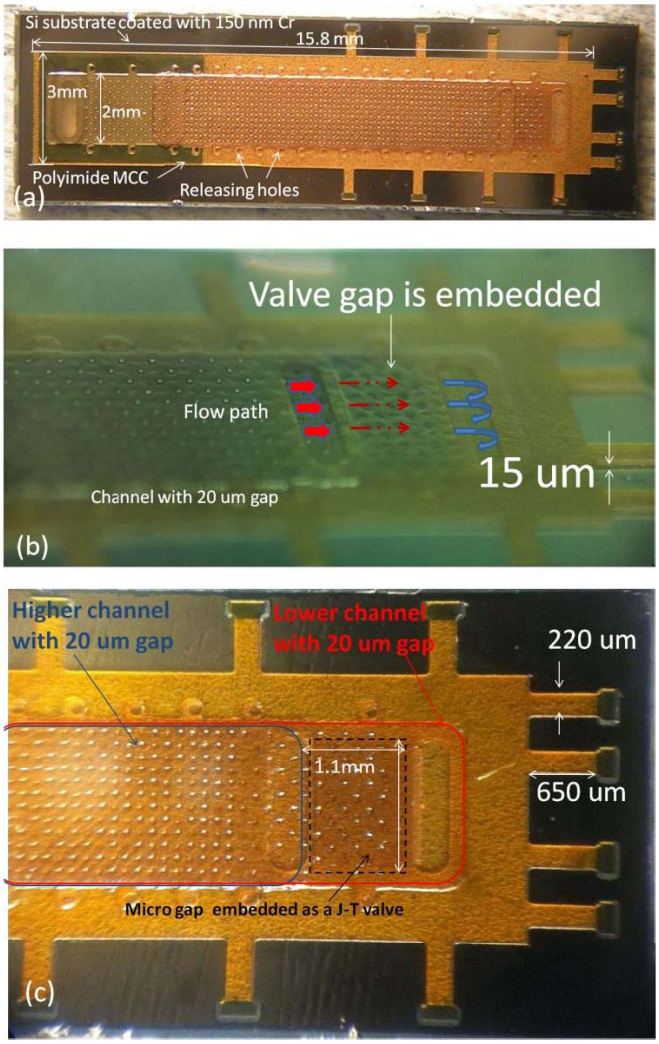

Fig. 8. Photos of the MCC after completing the batch process. (a) Top view of the MCC; (b) perspective view of the cold tip; (c) close-up top view of the cold tip.

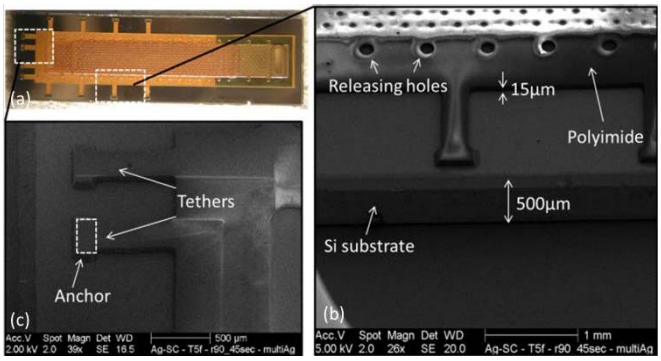

Fig. 9. Photos of the MCC after the batch process. (a) Top view of the MCC; (b) perspective view of the cold tip; (c) close-up top view of the cold tip.

In a previous polymer-based MCC design [8], [9], DuPont PI-2574 was used as the structure material. Because of the thermal mismatch between the polyimide layers and silicon substrate, all the tethers in this design were broken after the metal releasing. In order to solve the problem, DuPont PI-2611 which has a similar coefficient of thermal expansion to silicon was chose to make this device. No tether breakage was found after the copper releasing of the device.

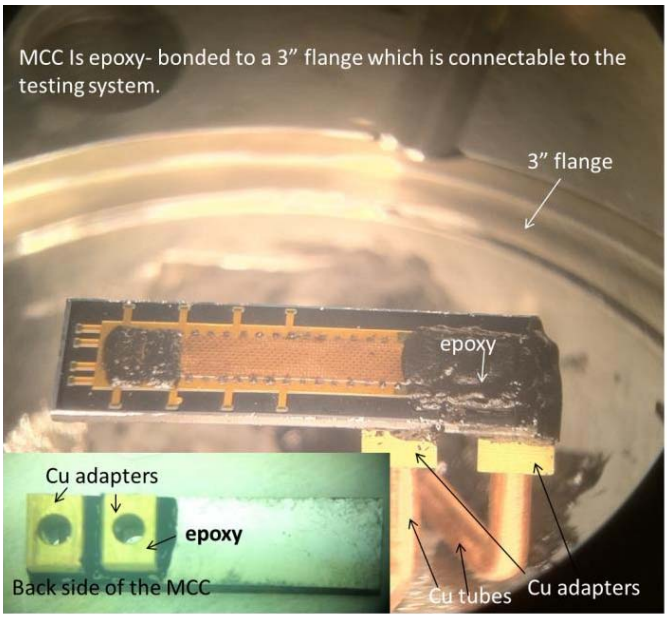

Fig. 10. Photos of MCC epoxy-bonded to copper tubes and connected to a 3 inches flange.

The process developed for this work to make the 3-D connected polymer channels has an extensive application to make a variety of polymer based micro-fluid systems. By using this process, one is able to make multilayers of channels and selectively connect them.

V. Cooling Test

To conduct the cooling test, the whole MCC assembly was epoxy-bonded to copper tubes and then connected to a macro stainless steel coupler (see Fig. 10). The coupler was compatible with a cooling test setup which includes a miniature compressor. The MCC was held in a vacuum of $<10^{-4}$ Torr during the cooling tests minimizing heat loads associated with conduction through air. Icing has been noted as a problem in MCCs [22], so to ensure that any trace amount of water in the refrigerant was removed, 1 g of 3 Å molecular sieve was placed in the test loop. A 15 μm particulates filter was installed between the molecular sieve and the MCC to prevent any particulate build-up in the micro-channels. The lines also experienced cycles of purging and evacuating with pure nitrogen to avoid potential smaller particles accumulation. Before running any tests, the lines were evacuated to a pressure of $<10^{-4}$ Torr, then charged with refrigerant from a low-pressure supply cylinder. A temperature sensor (Omega platinum resistance thermometer), with a footprint of 2 mm $\times$ 2 mm which allows good thermal contact was attached to the cold head using small amount of wax. As discussed in section III, aluminum tapes were used to cover most of the surface of the sensor in order to reduce the radiation loss. The resistance was monitored by applying a small voltage and measuring the current-draw. A miniature oil-free compressor composed of a miniature piston oscillator and micro-machined check valve assembly was use to deliver the refrigerant [23]. Temperature started to drop once the compressor was turned on.

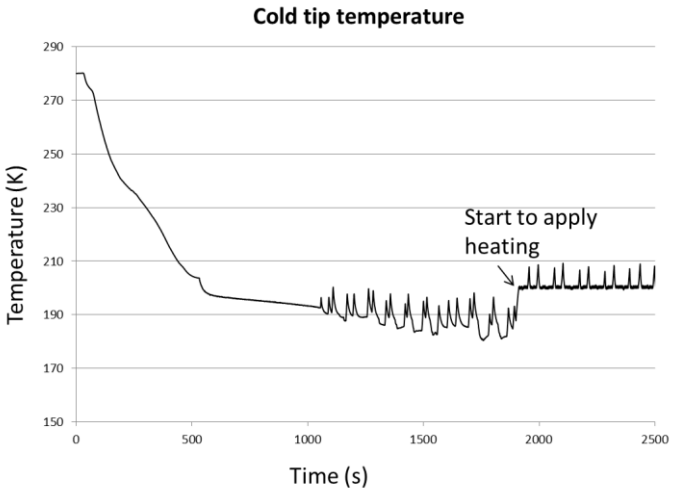

Fig. 11. Curves of cooling result. The cold tip was able to reach to a stable temperature of about 190 $\pm$ 10 K.

In macro-scaled Joule-Thomson refrigeration systems, mixed refrigerants have been widely applied to enhance the efficiency and refrigeration power. Radebaugh [10], Missimer [24], and Boiarski [25] reviewed recent developments and history of mixed refrigerants. Fuderer and Andrija [26] first used mixed gases in a single stream without phase separators in 1969. They found that the mixtures experienced mostly two-phase flow in the heat exchanger. As a result, boiling and condensing heat transfer of two-phase flow greatly enhanced cooling efficiency. The mixed refrigerant used was optimized by the program NIST4 [27] to maximize $(\Delta h|T)_{min}$ in the range of 300 K to 200 K with a high pressure of 4.0 bar and a low pressure of 1.0 bar. The minimum isothermal enthalpy difference is 4.09 kJ/mol in the temperature range from 300 K to 200 K. During the test, the base and inlet of the cold stage is pre-cooled in the ice and water bath to cool the inlet mixture to be about 280 K. During the testing, some component, e.g. pentane, was supposed to be liquefied at room temperature at high pressure, e.g. 6.2 bar in our test, and condensed and then held in the large tube of the system. In such a case the actual mixture that passed through the cooler had been changed to one that has a much lower enthalpy difference (as much as 10$\times$ lower) [28]. This can happen until the condensed liquid amount reaches a critical level to send pulses of liquid through the heat exchanger [29]. These liquid pulses result in oscillations in pressure, flow-rate, and temperature, as seen in Figs. 11–13 after roughly 1100 s. The pre-cooling here was thus to accelerate the system to reach the critical liquid level, otherwise it could take a long time to start start effective cooling.

The cooling result is shown in Fig. 11. The cold tip was able to reach a stable temperature of about 190 $\pm$ 10 K while the compressor is operated at a pressure ratio of 6.2 bar: 1.1 bar (see Fig. 12). The reason that the pressure is higher is that we have limited active controlling of the compressor because the piston has only two operation frequencies and 6.2 bar is the closest pressure we have to 4 bar which is the designed pressure. However, future work, e.g. adding active valves on both sides of the compressor, can be done to allow us to control the pressures actively.

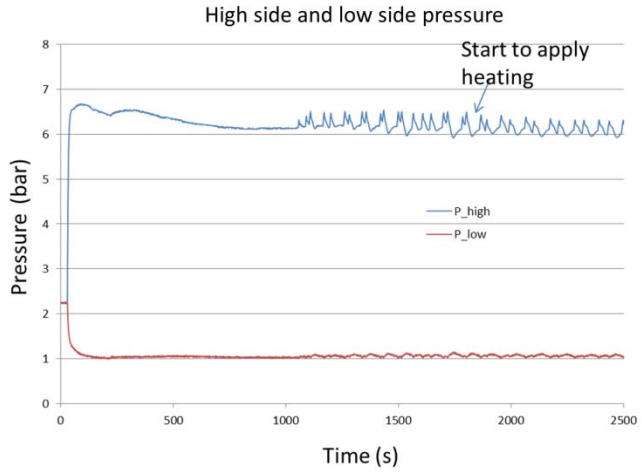

Fig. 12. Curves of pressure of each side of the compressor, the highest compression ratio reached is about 6.2:1bar. Pressures fluctuate according to the flow rate.

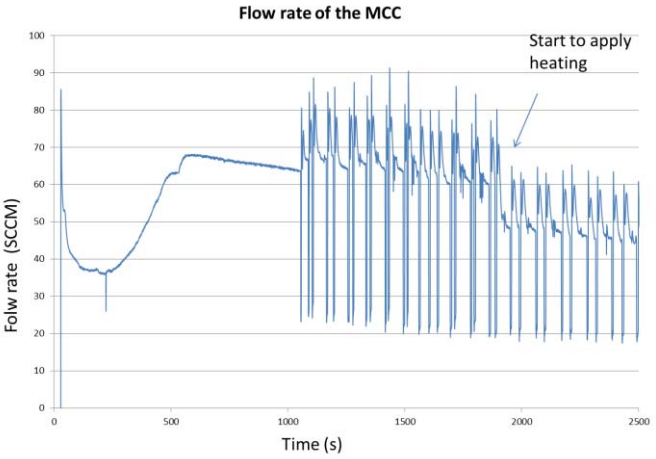

Fig. 13. Curve of the flow rate vs. time; flow rate kept increasing when the temperature was decreasing; the flow rate start to fluctuate when the temperature reached the 190 K.

The flow rate during the testing averaged about 62 sccm (see Fig. 13). We have also applied switched heating in order to make the temperature more stable and measure the heat lift. The switched heat was applied to the cold tip with the Omega platinum resistance thermometer. Once the temperature is below 200 K, 20 mW heating was then applied automatically as controlled by the computer. The temperate was then stabilized at about 200 K. The average heat applied was calculated to be about 5.2 mW indicating the heat lift is 5.2 mW at 200 K. After applying heat, the flow rate decreased to about 49 sccm according to the change of the viscosity and density of the mixture components.

The cooling temperature demonstrated by using the 300 K–200 K mixture successfully reached the optimized temperature. However, the net heat lift was still lower than what we had expected (12 mW). In terms of operation condition, the flow rate was higher than that designed (actual: 62 sccm; designed: 10 sccm) and pressures were also higher than that designed (actual: 6.2 : 1.1 bar; designed: 4 : 1 bar). The higher flow-rate and higher pressures ratio provided higher gross refrigeration however, the heat exchanger efficiency was thus degraded due to a large flow-rate. Another potential problem was that the enthalpy difference of the mixture in the optimization was under the assumption of a thoroughly mixed refrigerant. However, due to the liquid vapor separation issue, the enthalpy difference was smaller than the one calculated that also contributed to the reduced refrigeration. In addition, the heat exchanger tested had no metal shielding to cover its top surface. With an additional radiation shielding, the heat lift can be further improved.

VI. Conclusion

Monolithic polyimide MCCs have been designed and fabricated. With a five components refrigerant mixture, we successfully demonstrated the 200 K cooling with a 5.2 mW heat lift. This monolithic polyimide MCC did not encounter the mechanical leakage problem as the polyimide-based MCC reported in [9] since the soldered-interface is removed. It also enhanced the manufacturability and scalability of the MCC through the wafer-level processing. The lowest coldhead temperatures improved from 233 K to 190 K with a flow rate reduced from more than 260 sccm to about 62 sccm. By monolithically processing on wafer-level, the monolithic MCC is more compact, manufacturable, reliable and cost-effective.

Acknowledgment

The authors would like to thank the Defense Advanced Research Projects Agency of the Department of Defense for approving public release with distribution unlimited, and would also like to express their appreciation to Dr. Li-Anne Liew at NIST for discussion on some of the fundamental process problems and Dr. Marcia L. Huber for designing the mixed refrigerant

References

[1] M.-H. Lin, P. E. Bradley, H.-J. Wu, J. C. Booth, R. Radebaugh, and Y. C. Lee, "Design, fabrication, and assembly of a hollow-core fiber-based micro cryogenic cooler," in *Proc. Int. Solid-State Sens. Actuators Microsyst. Conf.*, Denver, CO, USA: Jun. 2009, pp. 1114–1117.

[2] R. Lewis, Y. Wang, J. Cooper, M. M. Lin, V. M. Bright, Y. C. Lee, *et al.*, "Micro cryogenic coolers for IR imaging," *Proc. SPIE*, vol. 8012, pp. 80122H-1–80122H-9, Apr. 2011.

[3] W. A. Little, "Microminiature refrigeration," *Rev. Sci. Instrum.*, vol. 55, no. 5, pp. 661–680, May 1984.

[4] S. Garvey, S. Logan, R. Rowe, and W. A. Little, "Performance characteristics of a low-flow rate 25 mW, LN_2 Joule–Thomson fabricated by photolithographic means," *Appl. Phys. Lett.*, vol. 42, no. 12, pp. 1048–1050, Mar. 1983.

[5] J. F. Burger, H. J. Holland, J. H. Seppenwoolde, E. Berenschot, H. J. M. ter Brake, J. G. E. Gardeniers, *et al.*, "165 K microcooler operating with a sorption compressor and a micromachined cold stage," in *Cryocoolers*, vol. 11. New York, NY, USA: Springer, 2002, pp. 551–560.

[6] P. P. P. M. Lerou, G. C. F. Venhorst, C. F. Berends, T. T. Veenstra, M. Blom, J. F. Burger, *et al.*, "Fabrication of micro cryogenic cold stage using MEMS-technology," *J. Micromech. Microeng.*, vol. 16, no. 10, pp. 1919–1925, Oct. 2006.

[7] M.-H. Lin, "Fabrication, assembly, and characterization of a hollow-core fiber-based micro cryogenic cooler," Ph.D. dissertation, Dept. Mech. Eng., Univ. Colorado, Boulder, CO, USA, 2009.

[8] Y. D. Wang, R. Lewis, M. Lin, R. Radebaugh, and Y. C. Lee, "Wafer-level processing for polymer-based planar micro cryogenic coolers," in *Proc. IEEE MEMS*, Paris, France, Feb. 2012, pp. 341–344.

[9] Y. D. Wang, R. Lewis, M. M.-H. Lin, R. Radebaugh, and Y. C. Lee, "The development of polymer-based planar micro cryogenic coolers," *J. Microelectromech. Syst.*, vol. 22, no. 1, pp. 244–252, Feb. 2013.

[10] R. Radebaugh, "Recent developments in cryocoolers," in *Proc. 19th Int. Congr. Refrigerat.*, The Hague, The Netherlands, 1995, pp. 973–989.
[11] R. Radebaugh, "Microscale heat transfer at low temperatures," in *Microscale Heat Transfer—Fundamentals and Applications*, vol. 193. New York, NY, USA: Springer, 2005, pp. 93–124.
[12] W. A. Little, "Microminiature refrigeration," in *Proc. AIP Conf. Adv. Cryogen. Eng., Trans. CEC*, vol. 52. Melville, NY, USA, 2008, pp. 597–605.
[13] MMR Technologies, Inc. Mountain View, CA, USA. (2013, Apr. 5) [Online]. Available: http://www.mmr.com
[14] P. P. P. M. Lerou, H. J. M. ter Brake, J. F. Burger, H. J. Holland, and H. Rogalla, "Characterization of micromachined cryogenic coolers," *J. Micromech. Microeng.*, vol. 17, no. 10, pp. 1956–1960, Oct. 2007.
[15] H. S. Cao, H. J. Holland, C. H. Vermeer, S. Vanapalli, P. P. P. M. Lerou, M. Blom, *et al.*, "Micromachined cryogenic cooler for cooling electronic devices down to 30 K," *J. Micromech. Microeng.*, vol. 23, no. 2, pp. 025014-1–025014-6, Feb. 2013.
[16] J. P. Holman, *Heat Transfer*, 8th ed. New York, NY, USA: McGraw-Hill, 1996.
[17] NIST Material Measurement Laboratory. Boulder, CO, USA. (2013, Apr. 5) [Online]. Available: http://cryogenics.nist.gov/MPropsMAY/Polyimide%20Kapton/PolyimideKapton_rev.htm
[18] E. Tschegg, "Mechanical properties and fracture behaviour of polyimide (SINTIMID) at cryogenic temperatures," *Cryogenics*, vol. 31, no. 10, pp. 878–883, Oct. 1991.
[19] H. Yokoyama, "Thermal conductivity of polyimide at cryogenic temperature," *Cryogenics*, vol. 35, no. 11, pp. 799–800, Nov. 1995.
[20] Y. W. Kim and M. G. Allen, "Surface micromachined platforms using electroplated sacrificial layers," in *Proc. Int. Conf. Solid-State Sens. Actuators*, San Francisco, CA, USA, Jun. 1991, pp. 651–654.
[21] Y. W. Kim and M. G. Allen, "Single- and multi-layer surface-micromachined platforms using electroplated sacrificial layers," *Sens. Actuators A, Phys.*, vol. 35, no. 1, pp. 61–68, Oct. 1992.
[22] P. P. P. M. Lerou, H. J. M. ter Brake, H. J. Holland, J. F. Burger, and H. Rogalla, "Insight into clogging of micromachined cryogenic coolers," *Appl. Phys. Lett.*, vol. 90, no. 6, pp. 064102-1–064102-3, Feb. 2007.
[23] R. Lewis, M. H. Lin, Y. Wang, J. Cooper, P. Bradley, R. Radebaugh, *et al.*, "Demonstration of an integrated micro cryogenic cooler and miniature compressor for cooling to 200 K," in *Proc. IMECE*, Denver, CO, USA, Nov. 2011, pp. 63908-1–63908-6.
[24] D. J. Missimer, *Auto-Refrigerating Cascade (ARC) Systems: An Overview*. New York, NY, USA: AIChE, 1995.
[25] M. J. Boiarski, V. M. Brodianski, and R. C. Longsworth, "Retrospective of mixed refrigerant technology and modern status of cryocoolers based on one-stage, oil-lubricated compressors," in *Advances in Cryogenic Engineering*, vol. 43. New York, NY, USA: Springer, 1998, pp. 1701–1708.
[26] M. Fuderer and A. Andrija, "Verfahren zur tieflqihlung," German Patent 1 426 956, 1969.
[27] *NIST Thermophysical Properties of Hydrocarbon Mixtures (SuperTrapp): Version 3.2*, Nat. Inst. Stand. Technol., Gaithersburg, MD, USA, 2007.
[28] R. J. Lewis, Y.-D. Wang, M.-H. Lin, M. L. Huber, R. Radebaugh, and Y. C. Lee, "Enthalpy change measurement of a mixed refrigerant in a micro cryogenic cooler in steady and pulsating flow regimes," *Cryogenics*, vol. 52, pp. 609–614, Aug. 2012.
[29] R. Lewis, Y. Wang, H. Schneider, Y. C. Lee, and R. Radebaugh, "Study of mixed refrigerants undergoing pulsating flow in micro coolers with pre-cooling," *Cryogenics*, vol. 57, pp. 140–149, Oct. 2013.

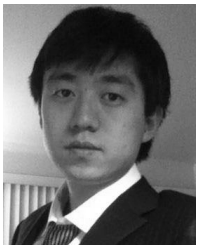

Yunda Wang received the B.Eng. degree in information engineering from Xi'an Jiaotong University, Xi'an, China in 2005; the M.Eng. degree in electronics and communication engineering from Peking University, Beijing, China in 2008; and the Ph.D. degree from University of Colorado, Boulder, in 2012.

He joined PARC, a Xerox company, in 2013 and is currently focusing on the development of a number of advanced MEMS structures for a novel refrigeration device. His research interests include the micro cryogenic cooling system and other novel microsystems for engineering applications, packaging and integration of electronic, M/NEMS, and RF MEMS devices, including micromechanical resonators, filters, and switches.

Ryan Lewis received the B.A. degree in physics from Whitman College, Walla Walla, in 2008, and the M.S. and Ph.D. degrees in mechanical engineering from the University of Colorado, Boulder, in 2010 and 2012, respectively.

He has served as a Technical Intern at Idaho National Lab and Pacific Northwest National Lab. He is currently a Post-Doctoral Research Associate at the University of Colorado, Boulder. His research interests include micro fluidics for cooling applications, multi-phase multi-component cryogenic refrigerants, and MEMS for thermal systems.

Ray Radebaugh received the B.S. degree in engineering physics from the University of Michigan, Ann Arbor, in 1962, and the M.S. and Ph.D. degrees in physics from Purdue University, West Lafayette, in 1965 and 1966, respectively.

He was the Group Leader of the Cryogenic Technologies Group for the National Institute of Standards and Technology (NIST) in Boulder, Colorado, from 1995 until his retirement from NIST in March, 2009. He continues to work for NIST half time under contract. From 1966 to 1968 he was an NRC-NIST Post-Doctoral Associate, and was a Staff Physicist with NIST after 1968 until his retirement.

In June, 2008, he was appointed an NIST Fellow. He has published over 160 papers as part of the open literature. He has received several awards, including the Department of Commerce Gold Medal in 2003, the Silver Medal in 1995, three best paper awards at Cryogenic Engineering Conferences, the R&D 100 Award in 1990 for the thermoacoustically driven pulse tube refrigerator, the J&E Hall Gold Medal in 1999 from the Institute of Refrigeration in England for his pioneering work on pulse tube refrigerators, and the 2009 Samuel C. Collins Award from the Cryogenic Engineering Conference for his contributions to cryogenics. He has been an invited speaker at numerous conferences, including the plenary speaker at the 1996 International Cryogenic Engineering Conference, the 1998 Applied Superconductivity Conference, the 2003 and 2008 International Conferences on Cryogenics and Refrigeration, and the 25th Low Temperature Physics Conference (2008).

Martin M.-H. Lin received the B.S. degree from National Taiwan University, Taipei, Taiwan, in 1995, and the M.S. and Ph.D. degrees from the University of Colorado, Boulder, in 2003 and 2009, respectively.

Prior to his Ph.D. study, he worked at Seagate Technology, Longmont, CO, in engineering, and AmTran Technology, Taipei, Taiwan, in business development. Currently, he is working on the chip-scale atomic clock (CSAC) at Symmetricom Inc., Beverly, MA. His research interests include the micro cryogenic cooling system design and fabrication, packaging and integration of electronic atomic-based sensors and M/NEMS, dynamic modeling of mechanical resonators, and other novel microsystems for engineering applications.

Victor M. Bright received the BSEE degree from the University of Colorado at Denver in 1986, and the M.S. and Ph.D. degrees from the Georgia Institute of Technology, in 1989 and 1992, respectively.

Dr. Bright is the Alvah and Harriet Hovlid Professor in the Department of Mechanical Engineering, College of Engineering and Applied Science, University of Colorado Boulder. From 2005 to 2007 he served as the Associate Dean for Research and from 2009 to 2013 he served as the Department Chair. Prior to joining the University of Colorado, he was a Professor in the Department of Electrical and Computer Engineering, Air Force Institute of Technology, Wright-Patterson Air Force Base, Ohio (1992-1997). During 2004, he was a Visiting Professor at the Swiss Federal Institute of Technology (ETH-Zurich), Switzerland. Dr. Bright's research activities include N/MEMS; silicon micromachining; microsensors/microactuators; optical, magnetic, and RF microsystems; atomic-layer deposited materials; N/MEMS reliability; and N/MEMS packaging. Dr. Bright has served on the Technical Program Committee of the IEEE MEMS 2000-2006 conferences, and as the General Co-Chair for the IEEE MEMS 2005 International Conference. He also served on the Technical Program Committees for the Transducers'03, Transducers'07, Transducers'13, IEEE/LEOS Optical MEMS 2003-2005, and Hilton Head 2008 Solid-State Sensors and Actuators Workshops. He was the Americas Technical Chair for Transducers 2013. Dr. Bright is a Fellow of ASME and a Senior Member of IEEE.

Yung-Cheng Lee received the B.S. degree from National Taiwan University, Taipei, Taiwan, in 1978, and the M.S. and Ph.D. degrees from the University of Minnesota, Minneapolis, in 1982 and 1984, respectively.

He was a Member of Technical Staff with AT&T Bell Laboratories, Murray Hill, NJ. He is currently a Professor of Mechanical Engineering at the University of Colorado at Boulder. His research activities include packaging and thermal management of multichip modules, 3-D packaging, self-aligning soldering, fluxless or solderless flip-chip connections, optoelectronics packaging, process control using fuzzy-logic models, MEMS, molecular biology integrated with micro/nanoscale technologies, and atomic layer deposition for integrated MEMS/NEMS. He was an Associate Editor of the ASME Journal of Electronic Packaging from 2001 to 2004.

Dr. Lee is an ASME Fellow. He was a Guest Editor for the IEEE TRANSACTION ON ADVANCED PACKAGING for two special issues on Packaging of MEMS/NEMS in 2003 and 2005. He was the recipient of a National Science Foundation Presidential Young Investigator Award in 1990.